



## A Study of the FitzHugh-Nagumo Model with Diffusion Term

Amattouch M.R.

**ABSTRACT:** This article aims to provide a theoretical background for the FitzHugh-Nagumo Model, which is a reaction-diffusion system originating from the field of neuroscience modeling. The paper begins by examining a linear reaction-diffusion system, establishing conditions under which the Hopf bifurcations exist. Thereafter, it bridges these findings to the nonlinear and nonhomogeneous FitzHugh-Nagumo (nhFHN) system, demonstrating the conditions necessary for generating oscillatory behavior in this system. Finally, numerical simulations of the nhFHN system was presented.

**Key Words:** FitzHugh-Nagumo Model, Hopf bifurcations, non-linear reaction diffusion equation.

### Contents

<b>1 Introduction</b>	<b>1</b>
<b>2 The Linear Model</b>	<b>2</b>
2.1 The Continuous Model . . . . .	2
2.2 The Discrete Model . . . . .	5
<b>3 The Nonlinear Equation</b>	<b>7</b>
3.1 The Fixed Points . . . . .	7
<b>4 Equations and Fixed Points</b>	<b>9</b>
4.1 System Description . . . . .	9
4.2 Fixed Points . . . . .	10
4.3 Jacobian Matrix and Eigenvalues . . . . .	10
4.4 Stability Conditions . . . . .	11
<b>5 Theorems and Remarks</b>	<b>11</b>
5.1 Theorems . . . . .	11
5.2 Remarks . . . . .	11
<b>6 Numerical Simulation</b>	<b>11</b>
6.1 Case Where Equation (4.4) Has One Real Solution . . . . .	12
6.2 Case Where Equation (4.4) Has Three Real Solutions . . . . .	14
<b>7 Conclusion</b>	<b>17</b>

### 1. Introduction

The nonlinear and nonhomogeneous FitzHugh-Nagumo (nhFHN) system is described by the equations below:

$$\begin{cases} \frac{\partial u}{\partial t} = u - \frac{u^3}{3} - v - \Delta u + J; \text{ in } \Omega \\ \varepsilon \frac{\partial v}{\partial t} = u - bv + a; \text{ in } \Omega \\ u = u_0; \text{ for } t = 0 \\ v = v_0; \text{ for } t = 0 \end{cases} \quad (1.1)$$

Here,  $u$  and  $v$  satisfy Neumann boundary conditions on the domain  $\Omega$ .  $J$  represents the density current, while  $b$ ,  $\varepsilon$ , and  $a$  are positive constants.

The linear model derived from this equation is described below:

$$\begin{cases} \frac{\partial u}{\partial t} &= u - v - \Delta u; \text{ in } \Omega \\ \varepsilon \frac{\partial v}{\partial t} &= u - bv; \text{ in } \Omega \\ u &= u_0; \text{ for } t = 0 \\ v &= v_0; \text{ for } t = 0 \end{cases} \quad (1.2)$$

Consequently, these equations are of significant interest in various scientific domains, such as Chemistry and Biology, particularly in the context of pattern formation [16,17]. The origin of these partial differential equations can be traced back to Hodgkin and Huxley (HH), who received the Nobel Prize in Physiology and Medicine in 1963 for their seminal model describing the propagation of electrical pulses along the giant squid neuron axon [1]. Their model involves a complex set of four ordinary differential equations [2,3]. A simplification of the HH model is the nhFHN model, which replicates oscillatory behavior [4].

Numerous qualitative analysis have been conducted on the FitzHugh-Nagumo model, addressing issues such as existence, local and global stability of traveling waves in the FHN model (see [7,8,9] and [10,11,5,6] for more details). These analysis either work in an unbounded domain or focus on singular aspects of the equation. In this work, we study the nhFHN model on any bounded domain by using the spectral decomposition of the Laplacian considered in [12,13]. We first treated a linear model derived from the nhFHN model. By projection onto the eigenfunctions of the Laplacian operator, we provided conditions for the existence of traveling waves. Next, we found similar results while considering the discrete Laplacian result of discretizing the Laplacian by a finite difference scheme. In the next section, we use the discrete Laplacian in the nhFHN model and propose assumptions about the dynamics of this partial differential equation. Finally, we presented numerical simulations that validate our results.

Please note that we do not address the existence and uniqueness of solutions for the equation treated here because it has also been done, see for example [14,15,16].

Since the same work could be applied to multidimensional domains, we take the domain  $\Omega = [0, 1]$  for simplicity throughout the entire article. It is important to note that for any multidimensional and complex domain, we would prefer to use a finite element method rather than a finite difference method to discretize the Laplacian because it is more suitable and consistent. However, our study could be adjusted to the case of finite element discretization.

## 2. The Linear Model

### 2.1. The Continuous Model

In this section, we consider the one-dimensional case with Neumann boundary conditions and the domain  $\Omega = [0, 1]$ . Therefore, it's important to note that the same proofs and theory can be applied to any domain and to the two or three-dimensional case.

The linear model is described by the following equations:

$$\begin{cases} \frac{\partial u}{\partial t} &= u - v - \Delta u; \text{ in } \Omega \\ \varepsilon \frac{\partial v}{\partial t} &= u - bv \text{ in } \Omega \\ u &= u_o \text{ for } t = 0 \\ v &= v_o \text{ for } t = 0 \end{cases} \quad (2.1)$$

It is well-known that the eigenvalues of the operator  $-\Delta u$  with Neumann boundary conditions form an orthonormal basis in  $L_2$ , with associated discrete eigenvalues  $(\lambda_k)_{k \in \mathbb{N}}$ . These eigenvalues satisfy  $\lambda_0 < \lambda_1 < \dots < \lambda_n < \dots$ , and it holds that  $\lim_{n \rightarrow \infty} \lambda_n = \infty$ . In the case of the square domain  $\Omega = [0, 1]$ , the eigenfunctions are given by  $\varphi_k(x) = \cos(k\pi x)$ , and the corresponding eigenvalues are expressed as  $\lambda_k = k^2\pi^2$ .

By utilizing spectral decomposition, we can express  $u(x, t)$  and  $v(x, t)$  as follows:

$$u(x, t) = \sum_{i=0}^{\infty} u_i(t) \varphi_i(x) \quad \text{and} \quad v(x, t) = \sum_{i=0}^{\infty} v_i(t) \varphi_i(x).$$

By performing calculations on problem (2.1), the following set of equations was obtained for each eigenmode  $k$ :

$$E_k : \begin{cases} \frac{\partial u_k}{\partial t} &= u_k - v_k - \sigma \lambda_k u_k \\ \frac{\partial v_k}{\partial t} &= \frac{1}{\varepsilon}(u_k - b v_k) \end{cases} \quad (2.2)$$

The ordinary differential equation obtained for each eigenmode  $k$  leads to the computation of the trace and determinant of the associated matrix  $A_k$ :

$$\text{tr}(A_k) = 1 - \lambda_k - \frac{b}{\varepsilon} \quad \text{and} \quad \det(A_k) = \frac{1}{\varepsilon}(1 - b(1 - \lambda_k)).$$

Since  $\text{tr}(A_k) \rightarrow -\infty$  and  $\det(A_k) \rightarrow +\infty$ , the unique stability condition for all systems  $E_k$  is  $\text{tr}(A_k) < 0$  and  $\det(A_k) > 0$  for all  $k$ , which implies  $1 - \frac{b}{\varepsilon} < 0$  and  $1 - b > 0$  or  $\varepsilon < b < 1$ . Therefore, we define  $\sigma_1$  and  $\sigma_2$  as follows:

$$\sigma_1 = 1 + \frac{b}{\varepsilon} + \frac{2}{\sqrt{\varepsilon}} \quad \text{and} \quad \sigma_2 = 1 + \frac{b}{\varepsilon} - \frac{2}{\sqrt{\varepsilon}}.$$

The fixed point is a spiral point if  $\text{tr}(A_k)^2 - 4\det(A_k) < 0$ , so

$$(1 - \lambda_k - \frac{b}{\varepsilon})^2 - \frac{2}{\varepsilon}(1 - b(1 - \lambda_k)) \Leftrightarrow (1 - \lambda_k + \frac{b}{\varepsilon} - \frac{2}{\sqrt{\varepsilon}})(1 - \lambda_k + \frac{b}{\varepsilon} + \frac{2}{\sqrt{\varepsilon}}) < 0 \Leftrightarrow (\lambda_k - \sigma_k^1)(\lambda_k - \sigma_k^2) < 0.$$

When  $\lambda_k$  crosses from right to left  $\sigma_1$  and  $\sigma_2$ ,  $\text{tr}(A_k)^2 - 4\det(A_k)$  changes sign from positive to negative.

This leads to the following theorems:

**Theorem 2.1** *We assume that  $\varepsilon < b < 1$ . Then, for each  $k$  large enough, there exists a value  $\sigma_1$  (and  $\sigma_2$  if  $b > 2\sqrt{\varepsilon} - \varepsilon$ ) such that as  $\lambda_k$  crosses  $\sigma_1$  from right to left, the 2D ODE associated system ( $E_k$ ) features a bifurcation from a sink to a spiral point. Furthermore, there is at most a finite number of systems ( $E_k$ ) for which  $(0, 0)$  is not a sink. In addition, the solution of problem (1.2) verifies the following:*

$$\lim_{t \rightarrow \infty} \|(u(t), v(t))\|_{L^2} = 0.$$

**Proof:** We use the same proof shown as in the articles [19,20]. □

Subsequently, we utilize an explicit Euler method to numerically solve Equation 2.1 with a time step of  $\Delta t = 0.001$  and a mesh size of  $h = 0.1$ . The method was implemented using the Scilab software. Several tests have been conducted to validate the results predicted by the theorem.

Figures 2 ( $u(0.2)$  in red and  $v(0.2)$  in blue) and 3 ( $v(0.2)$  as a function of  $u(0.2)$ ) depict an example that illustrates the behavior of the solution over time, which aligns with the conclusions drawn from the theorem. The initial conditions are set as  $u_{\text{init}}$  (1) which is a random value in the interval  $[0, 1]$  and  $v_{\text{init}} = 1$ . We take  $\varepsilon = 0.1$  and  $b = 0.1$ . The number of iterations is expressed as  $n = 2000000$ . As can be seen, the solutions tend to extinction as predicted.

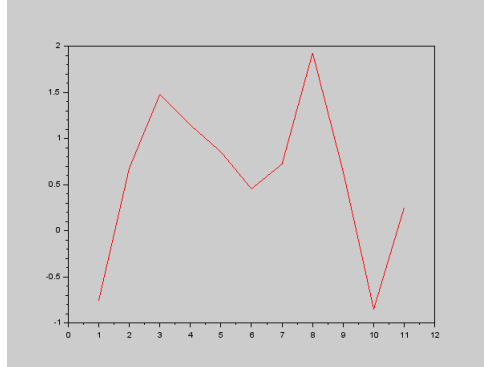


Figure 1: The concentration  $u$  in the initial value.

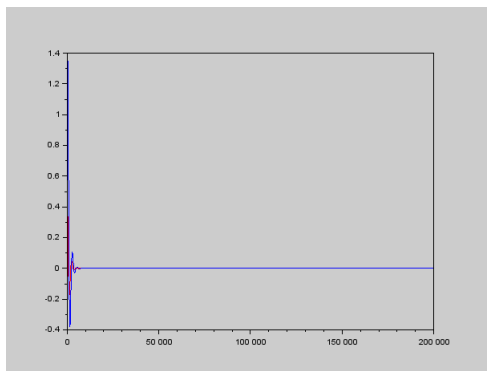


Figure 2: The concentration  $u(0.2)$  and  $v(0.2)$  over time.

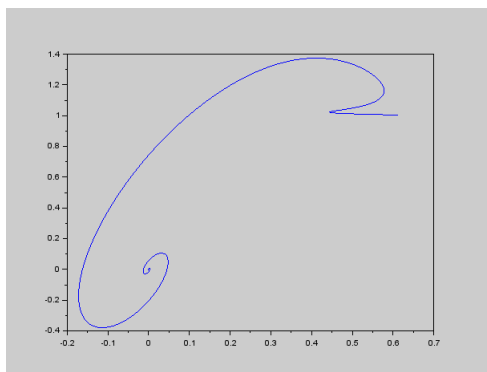


Figure 3: The concentration  $v(0.2)$  as a function of  $u(0.2)$ .

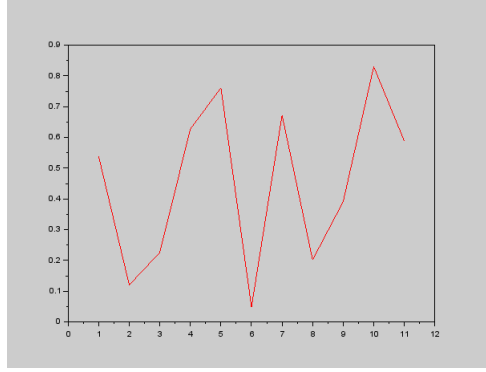
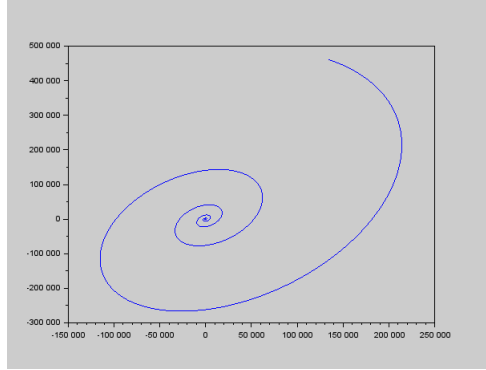
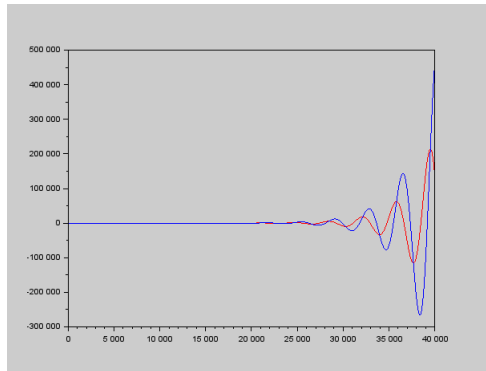
**Theorem 2.2** *Suppose that we don't have the condition  $\varepsilon < b < 1$ . Suppose that the initial condition is not the origin; then  $(0,0)$  is an unstable point for problem (1.2), and the solutions can be verified as shown below:*

$$\lim_{t \rightarrow \infty} \|(u(t), v(t))\|_{L^2} = \infty.$$

Notice that when  $\varepsilon$  and  $b$  change, the problem (1.2) changes its behavior. Also the system produces a Hopf bifurcation.

We utilize an explicit Euler method to numerically solve Equation (2.1) with a time step of  $\Delta t = 0.001$  and a mesh size of  $h = 0.1$ . Thus, the method is implemented using the Scilab software. Also, several tests have been conducted to validate the results predicted by the theorem.

Figures 5 ( $u(0.2)$  in red and  $v(0.2)$  in blue) and 6 ( $v(0.2)$  as a function of  $u(0.2)$ ) depict an example illustrating the behavior of the solution over time, which aligns with the conclusions drawn from the theorem. The initial conditions are set as  $u_{\text{init}}$  (Equation 1) is a normally random value in the interval  $[0, 1]$ , and  $v_{\text{init}}$  is uniformly random in space (Figure 4). We take  $\varepsilon = 0.3$  and  $b = 0.1$ . The number of iterations is  $nn = 40000$ . As can be seen, the solution explodes to infinity.

Figure 4: The concentration  $v$  in its initial value.Figure 5: The concentration  $u(0.2)$  and  $v(0.2)$  over time.Figure 6: The concentration  $v(0.2)$  as a function of  $u(0.2)$ .

## 2.2. The Discrete Model

We partition the domain in space using a mesh  $x_0, \dots, x_N$ . We assume a uniform spatial partition, where the difference between two consecutive points is denoted as  $h = \Delta x$ .

The points are represented as  $u(x_j, t) = u_j(t)$ , and the explicit scheme for problem (4.1) is given by

the following system of equations:

$$\begin{cases} \frac{\partial u_i}{\partial t} &= u_i^n - v_i^n + \frac{u_{i+1}^n + u_{i-1}^n - 2u_i^n}{h^2} \\ \frac{\partial v_i}{\partial t} &= \frac{1}{\varepsilon}(u_i^n - bv_i^n) \end{cases} \quad (2.3)$$

Due to Neumann condition, we take  $u_{-1} = u_0$  and  $u_{N+1} = u_N$ . This system can be expressed in matrix form as:

$$\frac{\partial U}{\partial t} = AU.$$

Where

$$A = \begin{pmatrix} A_1 & -I_N \\ \frac{1}{\varepsilon}I_N & -\frac{b}{\varepsilon}I_N \end{pmatrix}.$$

And

$$U = \begin{pmatrix} u_1 \\ \vdots \\ u_N \end{pmatrix}.$$

The matrix  $A$  can be decomposed into two submatrices:

$$A_1 = \begin{pmatrix} 1 + \frac{2}{h^2} & -\frac{1}{h^2} & 0 & \dots & 0 \\ -\frac{1}{h^2} & 1 + \frac{2}{h^2} & -\frac{1}{h^2} & & \vdots \\ 0 & \ddots & \ddots & \ddots & \vdots \\ \vdots & & & & \\ 0 & \dots & 0 & -\frac{1}{h^2} & 1 + \frac{2}{h^2} \end{pmatrix}.$$

The eigenvectors of the discrete Laplacian are given by:

$$V_k = \begin{pmatrix} \cos(k\pi h) \\ \cos(2k\pi h) \\ \vdots \\ \cos(kN\pi h) \end{pmatrix},$$

associated with the eigenvalue:

$$\lambda_k = -\frac{4 \sin^2(kh\pi/2)}{h^2}.$$

From this, we can deduce the eigenvalues of the matrix  $A$  as:  $\alpha_k^m$  for  $m = 1, 2$ , where  $\alpha_k^i$  is the solution to the equation:

$$x^2 + \left(\frac{b}{\varepsilon} - \lambda_k - 1\right)x + \frac{1}{\varepsilon}(1 - b\lambda_k + b) = 0.$$

The matrix  $A$  is nonsingular, meaning all its eigenvalues are nonzero. Therefore, the unique stationary point of the system (2.3) is the zero vector.

Furthermore, all eigenvalues of  $A$  are real. Using the same computations as in 4.1, we can deduce the following:

- If  $\varepsilon < b < 1$ , all eigenvalues are negative, indicating that the zero vector is a sink. In this case,

$$\lim_{t \rightarrow \infty} \sum_{i=0}^N u_i^2 + v_i^2 = 0.$$

- If  $\varepsilon < b < 1$ , there exists at least one positive eigenvalue, indicating that the zero vector is a saddle point. In this case,

$$\lim_{t \rightarrow \infty} \sum_{i=0}^N u_i^2 + v_i^2 = +\infty.$$

Since the discrete Laplacian converges uniformly to the continuous Laplacian [15,21], we have proven Theorems 1, 2, and 3 as stated in Section 4.1.

### 3. The Nonlinear Equation

#### 3.1. The Fixed Points

In this section, we consider the following nonlinear equation:

$$\begin{cases} \frac{\partial u}{\partial t} = u - v - \frac{1}{3}u^3 + \frac{\partial^2 u}{\partial x^2} + J & \text{on } \Omega \\ \frac{\partial v}{\partial t} = \frac{1}{\varepsilon}(u - bv + a) & \text{on } \Omega \\ u(0, x) = h_0 \\ \frac{\partial u}{\partial x}(t, 0) = \frac{\partial u}{\partial x}(t, 1) = \frac{\partial v}{\partial x}(t, 0) = \frac{\partial v}{\partial x}(t, 1) = 0 \end{cases} \quad (3.1)$$

We discretize the Laplacian as follows:

$$\frac{\partial^2 u}{\partial x^2} \approx \frac{u_{i+1} + u_{i-1} - 2u_i}{h^2},$$

where  $h$  is the mesh size. By substituting this approximation into problem (3.1), we obtain the following vectorial dynamical equation:

$$\begin{cases} \frac{\partial u_i}{\partial t} = u_i - v_i - \frac{1}{3}u_i^3 + \frac{u_{i+1} + u_{i-1} - 2u_i}{h^2} + J \\ \frac{\partial v_i}{\partial t} = \frac{1}{\varepsilon}(u_i - bv_i + a) \end{cases} \quad \text{for } i = 0, \dots, N. \quad (3.2)$$

The stationary points of equation (3.2) satisfy the following equations for  $i = 2, \dots, N-1$ :

$$u_i - v_i - \frac{1}{3}u_i^3 + \frac{u_{i+1} + u_{i-1} - 2u_i}{h^2} + J = 0 \quad (3.3)$$

$$u_i - bv_i + a = 0. \quad (3.4)$$

We substitute  $v_i = \frac{1}{b}(u_i - a)$  of equation (3.4) in equation of (3.3), we obtain:

$$(1 - \frac{1}{b})u_i - \frac{1}{3}u_i^3 + \frac{u_{i+1} + u_{i-1} - 2u_i}{h^2} + J - \frac{a}{b} = 0.$$

Now we will prove  $(u_i)$  is constant:  $u_1 = u_2 = \dots = u_N$ .

Let  $v_i = u_i - u_{i+1}$ . By substitution in equation (3.4), we have:

$$(1 - \frac{1}{b})v_i - \frac{1}{3}v_i(u_i^2 + u_{i+1}^2 + u_i u_{i+1}) + \frac{v_{i+1} + v_{i-1} - 2v_i}{h^2} = 0.$$

By multiplying this equation (4.2) by  $v_i$  and summing  $i = 0, \dots, N-1$ , we obtain:

$$\sum_{i=0}^{N-1} (1 - \frac{1}{b})v_i^2 - \frac{1}{3}v_i^2(u_i^2 + u_{i+1}^2 + u_i u_{i+1}) + \frac{v_{i+1} + v_{i-1} - 2v_i}{h^2}v_i = 0.$$

Now, we know

$$\sum_{i=0}^{N-1} \frac{v_{i+1} + v_{i-1} - 2v_i}{h^2}v_i = - \sum_{i=0}^{N-1} \frac{(v_{i+1} - v_i)^2}{h^2}.$$

So,

$$\sum_{i=0}^{N-1} \left(1 - \frac{1}{b}\right) v_i^2 - \frac{1}{3} v_i^2 (u_i^2 + u_{i+1}^2 + u_i u_{i+1}) + - \sum_{i=0}^{N-1} \frac{(v_{i+1} - v_i)^2}{h^2} = 0.$$

By the inequality:

$$(v_{i+1} - v_i)^2 \leq 2(v_{i+1}^2 + v_i^2),$$

we have

$$\sum_{i=0}^{N-1} \left(1 - \frac{1}{b} - \frac{2}{h^2}\right) v_i^2 - \frac{1}{3} v_i^2 (u_i^2 + u_{i+1}^2 + u_i u_{i+1}) \geq 0.$$

Since  $h$  is small enough, we have  $1 - \frac{1}{b} - \frac{2}{h^2} < 0$  and  $u_i^2 + u_{i+1}^2 + u_i u_{i+1} > 0$ . Also, we deduce that we have necessarily  $v_i = 0$  for  $i = 0 \dots N-1$  because a sum of negative terms is positive if and only if the entire terms are null.

So  $v_i = 0$  for  $i = 0 \dots N-1$  then,  $u_0 = u_1 = \dots u_{N+1} = C$  where  $C$  is a constant solution of:

$$\left(1 - \frac{1}{b}\right)x - \frac{1}{3}x^3 + J - \frac{a}{b} = 0. \quad (3.5)$$

This equation has at least one solution. Notice  $D = 9(J - \frac{a}{b})^2 + 4(\frac{1}{b} - 1)^3$ . We have three cases:

- $D > 0$ , equation (4.4) has a unique solution and our system (3.2) has a unique stationary point.
- $D = 0$ , equation (4.4) has two solutions and our system (3.2) has two stationary points.
- $D < 0$  equation (4.4) has three solutions and our system (3.2) has three stationary points.

The solutions of equation (4.4) are given by the Cardano formula:

$$x = \sqrt[3]{\frac{J - \frac{a}{b} - \sqrt{D}}{2}} + \sqrt[3]{\frac{J - \frac{a}{b} + \sqrt{D}}{2}}.$$

Now, we will use the LaSalle theorem to prove the asymptotic stability of all the fixed points. We have for  $i = 1, \dots, N$ :

$$\frac{\partial u_i}{\partial t} = u_i - v_i - \frac{1}{3}u_i^3 + \frac{u_{i+1} + u_{i-1} - 2u_i}{h^2} + J \quad (3.6)$$

$$\varepsilon \frac{\partial v_i}{\partial t} = (u_i - bv_i + a). \quad (3.7)$$

$$(3.8)$$

By multiplying equation (3.6) by  $u_i$  and equation (3.7) by  $v_i$  for  $i = 0, \dots, N$ , we obtain:

$$\frac{\partial \frac{u_i^2}{2}}{\partial t} = u_i^2 - v_i u_i - \frac{1}{3}u_i^4 + \frac{u_{i+1} + u_{i-1} - 2u_i}{h^2} u_i + J u_i \quad (3.9)$$

$$\varepsilon \frac{\partial \frac{v_i^2}{2}}{\partial t} = u_i v_i - b v_i^2 + a v_i. \quad (3.10)$$

$$(3.11)$$

Summing equations (3.9) and (3.10):

$$\frac{\partial \frac{u_i^2}{2} + \varepsilon \frac{v_i^2}{2}}{\partial t} = u_i^2 + J u_i - b v_i^2 + a v_i - \frac{1}{3}u_i^4 + \frac{u_{i+1} + u_{i-1} - 2u_i}{h^2} u_i.$$



Taking the sum of these equations over  $i = 0, \dots, N$ , we have:

$$\begin{aligned}
& \frac{\partial \sum_{i=0}^N (\frac{u_i^2}{2} + \varepsilon \frac{v_i^2}{2})}{\partial t} = \\
& \sum_{i=0}^N (u_i^2 + Ju_i) + \sum_{i=0}^N (-bv_i^2 + av_i) - \sum_{i=0}^N \frac{1}{3} u_i^4 + \sum_{i=0}^N \frac{u_{i+1} + u_{i-1} - 2u_i}{h^2} u_i \\
& = \sum_{i=0}^N (u_i^2 + Ju_i) + \sum_{i=0}^N (-bv_i^2 + av_i) - \sum_{i=0}^N \frac{1}{3} u_i^4 - \sum_{i=0}^N \frac{u_{i+1} + u_{i-1} - 2u_i}{h^2} u_i \\
& \leq \sum_{i=0}^N (u_i^2 + Ju_i) + \sum_{i=0}^N (-bv_i^2 + av_i) - \sum_{i=0}^N \frac{1}{3} u_i^4.
\end{aligned} \tag{3.12}$$

Since  $Ju_i \leq 0.5u_i^2 + 0.5J^2$  and  $av_i \leq \frac{b}{2}v_i^2 + \frac{a^2}{2b}$ , we have:

$$\frac{\partial \sum_{i=0}^N (\frac{u_i^2}{2} + \varepsilon \frac{v_i^2}{2})}{\partial t} \leq \sum_{i=0}^N (\frac{3}{2} u_i^2) + \sum_{i=0}^N (-\frac{b}{2} v_i^2) - \sum_{i=0}^N \frac{1}{3} u_i^4 + (N+1)(\frac{J^2}{2} + \frac{a^2}{2b}). \tag{3.13}$$

And because  $\frac{1}{3}u_i^4 + 3 \geq 2u_i^2$ , we deduce:

$$\frac{\partial \sum_{i=0}^N (\frac{u_i^2}{2} + \varepsilon \frac{v_i^2}{2})}{\partial t} \leq - \sum_{i=0}^N (\frac{1}{2} u_i^2 + \frac{b}{2} v_i^2) + (N+1)(\frac{J^2}{2} + \frac{a^2}{2b} + 3).$$

Then, there exist two positive numbers  $\alpha$  and  $\beta$  such that:

$$\frac{\partial \sum_{i=0}^N (\frac{u_i^2}{2} + \varepsilon \frac{v_i^2}{2})}{\partial t} \leq -\alpha \sum_{i=0}^N (\frac{u_i^2}{2} + \varepsilon \frac{v_i^2}{2}) + \beta.$$

where  $\beta = (N+1)(\frac{J^2}{2} + \frac{a^2}{2b} + 3)$  and  $\alpha = \min(1, b)$ .

Since the quantity  $\sum_{i=0}^N (\frac{u_i^2}{2} + \varepsilon \frac{v_i^2}{2})$  acts as a norm, the LaSalle Invariance Principle ensures the asymptotic behavior of our system to be near the fixed points.

## 4. Equations and Fixed Points

### 4.1. System Description

In this section, we consider a system of two coupled partial differential equations, denoted as (4.1), which can be written as follows:

$$\begin{cases} \frac{\partial u}{\partial t} = u - v - \frac{1}{3}u^3 + \frac{\partial^2 u}{\partial x^2} & \text{on } \Omega \\ \frac{\partial v}{\partial t} = \frac{1}{\varepsilon}(u - bv) & \text{on } \Omega \end{cases} \tag{4.1}$$

Here,  $u(x, t)$  and  $v(x, t)$  represent the system variables,  $x$  and  $t$  denote the spatial and temporal coordinates,  $\Omega$  is the spatial domain, and  $\varepsilon, b$  are parameters.

## 4.2. Fixed Points

The fixed points of this system correspond to constant solutions, denoted as  $C$ , where  $C = u_0 = u_1 = \dots = u_N$ . These fixed points satisfy the following equations for  $i = 2, \dots, N-1$ :

$$u_i - v_i - \frac{1}{3}u_i^3 + \frac{u_{i+1} + u_{i-1} - 2u_i}{h^2} + J = 0 \quad (4.2)$$

$$u_i - bv_i + a = 0. \quad (4.3)$$

By substituting  $v_i = \frac{1}{b}(u_i - a)$  from equation (4.3) into equation (4.2), we obtain:

$$(1 - \frac{1}{b})u_i - \frac{1}{3}u_i^3 + \frac{u_{i+1} + u_{i-1} - 2u_i}{h^2} + J - \frac{a}{b} = 0.$$

We can deduce that the solution  $(u_i)$  is constant, i.e.,  $u_0 = u_1 = \dots = u_{N+1} = C$ , which satisfies:

$$(1 - \frac{1}{b})x - \frac{1}{3}x^3 + J - \frac{a}{b} = 0. \quad (4.4)$$

Depending on the discriminant  $D = 9(J - \frac{a}{b})^2 + 4(\frac{1}{b} - 1)^3$ , we have three cases:

- If  $D > 0$ , equation (4.4) has a unique solution, and the system (4.1) has a unique stationary point.
- If  $D = 0$ , equation (4.4) has two solutions, and the system (4.1) has two stationary points.
- If  $D < 0$ , equation (4.4) has three solutions, and the system (4.1) has three stationary points.

## 4.3. Jacobian Matrix and Eigenvalues

The Jacobian matrix associated with the dynamical equations (4.1), computed at  $U = \begin{pmatrix} u_1 \\ u_2 \\ \vdots \\ u_N \end{pmatrix}$ , is

given by:

$$A = \begin{pmatrix} (1 - C^2)I_N + A_1 & -I_N \\ \frac{1}{\varepsilon}I_N & -\frac{b}{\varepsilon}I_N \end{pmatrix}.$$

Here,  $A_1$  represents the discrete Laplacian submatrix:

$$A_1 = \begin{pmatrix} -\frac{2}{h^2} & \frac{1}{h^2} & 0 & \dots & 0 \\ \frac{1}{h^2} & -\frac{2}{h^2} & \frac{1}{h^2} & & \vdots \\ 0 & \ddots & \ddots & \ddots & \vdots \\ \vdots & & & & \\ 0 & \dots & 0 & \frac{1}{h^2} & -\frac{2}{h^2} \end{pmatrix}.$$

The eigenvalues  $\alpha_i^m$  of the Jacobian matrix  $A$  can be determined by solving:

$$x^2 + \left(\frac{b}{\varepsilon} - \lambda_i - 1 + C^2\right)x + \frac{1}{\varepsilon}(1 - b\lambda_i + b(1 - C^2)) = 0.$$

The real part of  $\alpha_i^m$ , denoted as  $\Re(\alpha_i^m)$ , plays a crucial role in determining the system's behavior.

#### 4.4. Stability Conditions

The asymptotic behavior of the solutions of equation (4.1) near the constant  $C$  is determined by the real part of the eigenvalues  $\alpha_i^m$ . Specifically, if  $\Re(\alpha_i^m) \leq 0$  for all  $i, m$ , then the system converges to the stationary point, and otherwise, it oscillates around it.

The stability conditions can be expressed as follows:

$$\Re(\alpha_i^m) \leq 0 \Leftrightarrow tr \leq 0 \text{ and } tr^2 - \Delta \geq 0.$$

Where:

$$tr = \frac{b}{\varepsilon} - \lambda_i - 1 + C^2.$$

And:

$$\Delta = tr^2 - \frac{4}{\varepsilon} (1 - b\lambda_i + b(1 - C^2)).$$

These conditions determine whether the system converges to the stationary point or oscillates around it.

### 5. Theorems and Remarks

#### 5.1. Theorems

Here, we present two theorems related to the asymptotic behavior of the system defined by equation 4.1:

**Theorem 5.1** *Let  $C$  be a solution of equation (4.4). If  $\frac{b}{\varepsilon} - 1 + C^2 \geq 0$  and  $1 - b(1 - C^2) \geq 0$ , then for all trajectories of equation (4.1) that are closer to the constant  $C$  than other solutions of (4.4). Thus, the system converges to the stationary point  $(C, \frac{1}{b}(C + a))$ . Furthermore, as  $t$  approaches infinity, we have:*

$$\lim_{t \rightarrow \infty} \| (u - C, v - \frac{1}{b}(C + a)) \| = 0.$$

**Theorem 5.2** *Let  $C$  be a solution of equation (4.4). Suppose the parameters  $a, b, \varepsilon$ , and  $C$  do not satisfy the conditions of Theorem 5.1. Then, for all trajectories of equation (4.1) that are closer to the constant  $C$  than other solutions of (4.4), the system will oscillate around the stationary point  $(C, \frac{1}{b}(C + a))$ , except for some initial conditions derived from the eigenvectors of the Laplacian.*

#### 5.2. Remarks

Several remarks related to the conditions and implications of the theorems are provided:

- Remark 1: If equation (4.4) has a unique solution, the behavior described in Theorems 5.1 and 5.2 is global.
- Remark 2: Under certain parameter conditions,  $1 - b + bC^2 \geq 0$  for any values of  $a, b$ , and  $J$ .
- Remark 3: The system exhibits a spiral behavior in infinity when  $\Delta < 0$ , which is true when  $\frac{2}{\sqrt{\varepsilon}} < \frac{b}{\varepsilon} + 1 + C^2 < \frac{2}{\sqrt{\varepsilon}} - 1$ .

### 6. Numerical Simulation

In this section, we present numerical simulations using Scilab. In 2D simulations, we used FreeFem [23], which is a finite element software [23] capable of solving partial differential equations.

To solve Equation (4.1), we employed an explicit Euler semi-implicit scheme with a time step of  $\Delta t = 10^{-3}$  and a spatial mesh size of  $h = 0.1$ . Here, we illustrate numerical simulations with different parameters:  $a, b, \varepsilon$ , and  $J$ , and explore different cases of solutions to Equation (4.4) with various behaviors.

### 6.1. Case Where Equation (4.4) Has One Real Solution

First, we consider the case where  $\frac{b}{\varepsilon} - 1 + C^2 \geq 0$ ,  $1 - b(1 - C^2) \geq 0$ , and  $\frac{b}{\varepsilon} + C^2 - \frac{2}{\sqrt{\varepsilon}} \approx 2.3232245 > 0$ . We set the following parameters:  $\varepsilon = 0.1$ ,  $a = 0.1$ ,  $b = 0.8$ , and  $J = 0.5$ . In this case,  $D = 9(J - \frac{a}{b})^2 + 4(\frac{1}{b} - 1)^3 > 0$ , and Equation 4.4 has a unique real solution  $C \simeq 0.8048477$  that satisfies  $\frac{b}{\varepsilon} - 1 + C^2 \simeq 7.167 \geq 0$  and  $1 + b(1 - C^2) \simeq 1.66 \geq 0$ .

Figures 7 and 8 confirm the result of Theorem 5.1, where the solution converges to a constant.

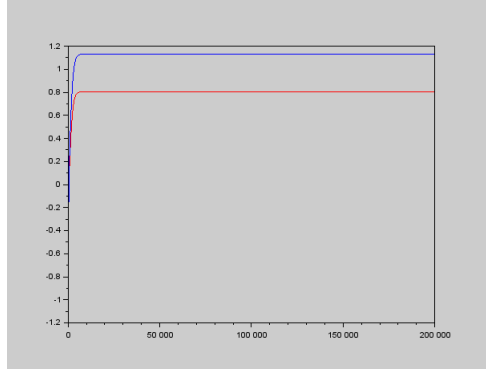


Figure 7: The concentration  $u(0.2)$  and  $v(0.2)$  over time

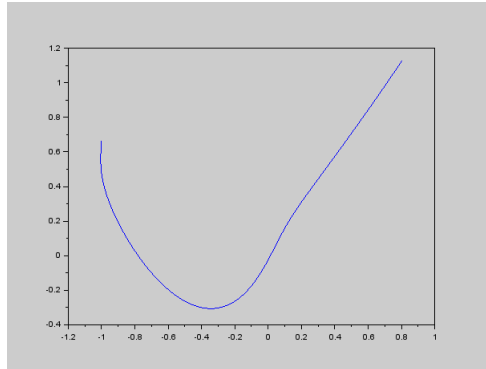
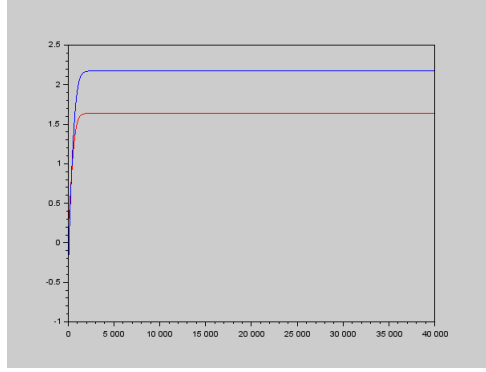
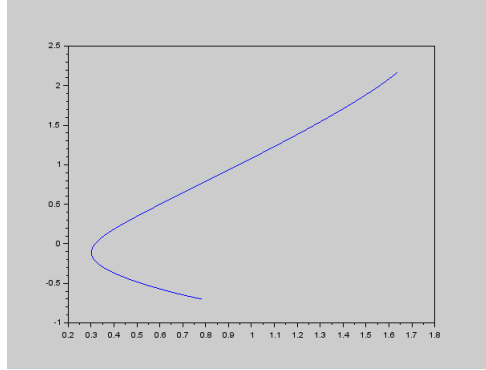


Figure 8: The concentration  $v(0.2)$  as a function of  $u(0.2)$

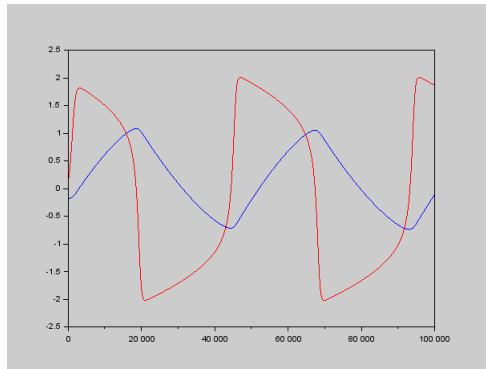
Next, we consider a case where  $\frac{b}{\varepsilon} - 1 + C^2 \geq 0$  and  $\frac{2}{\sqrt{\varepsilon}} > \frac{b}{\varepsilon} + 1 - C^2 > 1 - \frac{2}{\sqrt{\varepsilon}}$ . We set the parameters as follows:  $\varepsilon = 0.5$ ,  $a = 0.1$ ,  $b = 4$ , and  $J = 2$ . In this case,  $D = 9(J - \frac{a}{b})^2 + 4(\frac{1}{b} - 1)^3 > 0$ , and Equation 4.4 has a unique real solution  $C \simeq 12.2183194$  that satisfies  $\frac{b}{\varepsilon} - 1 + C^2 \geq 0$  and  $1 + b(1 - C^2) \geq 0$ .

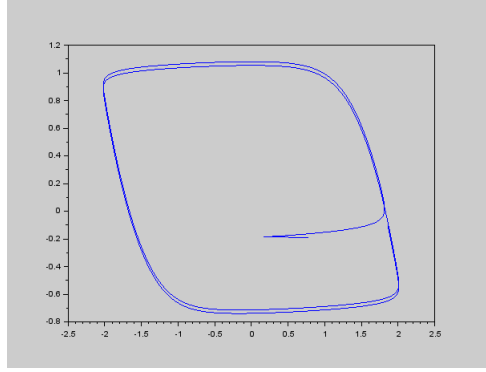
Figures 9 and 10 confirm the result of Theorem 5.1, where the solutions converge to a constant.

Figure 9: The concentration  $u(0.2)$  and  $v(0.2)$  over timeFigure 10: The concentration  $v(0.2)$  as a function of  $v(0.2)$ 

Now, let's treat the case where  $\frac{b}{\varepsilon} - 1 + C^2 < 0$ . We set the parameters as follows:  $\varepsilon = 20$ ,  $a = 0.1$ ,  $b = 0.1$ , and  $J = 0.01$ . In this case,  $D = 9(J - \frac{a}{b})^2 + 4(\frac{1}{b} - 1)^3 > 0$ , and Equation 4.4 has a unique real solution  $C \simeq u = -0.1099508$  that satisfies  $\frac{b}{\varepsilon} - 1 + C^2 \simeq -0.9829108 < 0$ .

Figures 11 and 12 confirm the result of Theorem 5.2, where the solutions oscillate in infinity.

Figure 11: The concentration  $u(0.2)$  and  $v(0.2)$  over time

Figure 12: The concentration  $v(0.2)$  as a function of  $v(0.2)$ 

### 6.2. Case Where Equation (4.4) Has Three Real Solutions

We consider a case where Equation (4.4) has three real solutions:  $C_1 \simeq 0$ ,  $C_2 = 1.2247449$ , and  $C_3 = 1.2247449$ . We set the parameters as follows:  $\varepsilon = 0.1$ ,  $a = 1$ ,  $b = 2$ , and  $J = 0.5$ . In this case,  $D = 9(J - \frac{a}{b})^2 + 4(\frac{1}{b} - 1)^3 < 0$ , and only  $C_2$  and  $C_3$  satisfy  $\frac{b}{\varepsilon} - 1 + C^2 \geq 0$  and  $1 + b(1 - C^2) \geq 0$ . Figure 13 and 14 confirm the result of Theorem 5.1, where the solution  $u$  converges to a constant  $C_3$ .

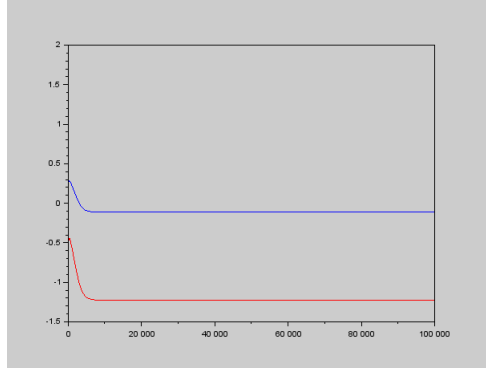
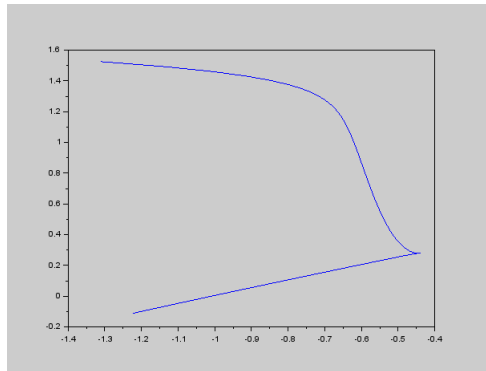
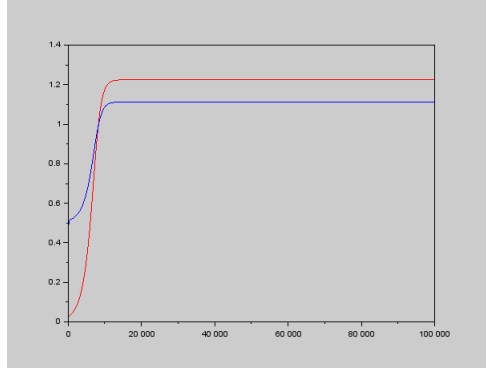
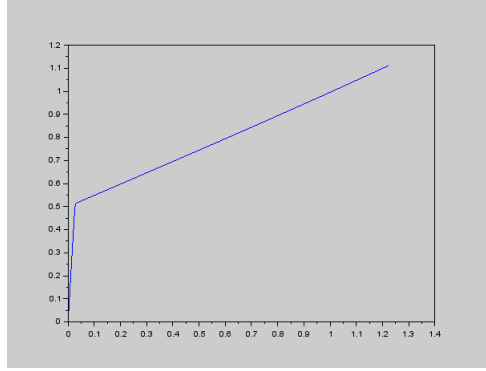
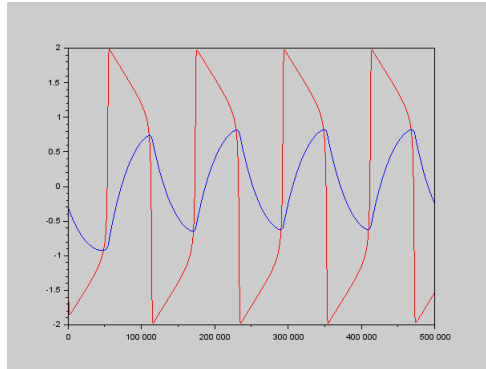
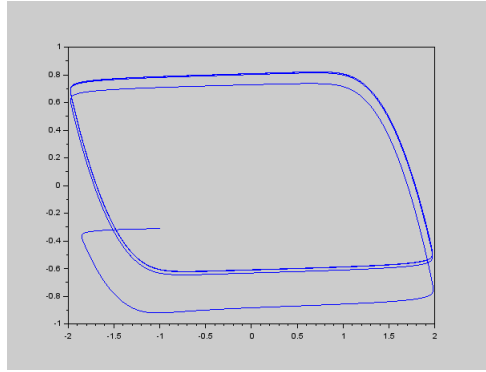
Figure 13: The concentration  $u(0.2)$  and  $v(0.2)$  over timeFigure 14: The concentration  $v(0.2)$  as a function of  $v(0.2)$ 

Figure 15 and 16 confirm the result of Theorem 5.1, where the solution  $u$  converges to a constant  $C_2$  because the initial condition  $U_{init} = 0$  and  $V_{init} = 0$  is closer to  $C_2$  than  $C_3$ .

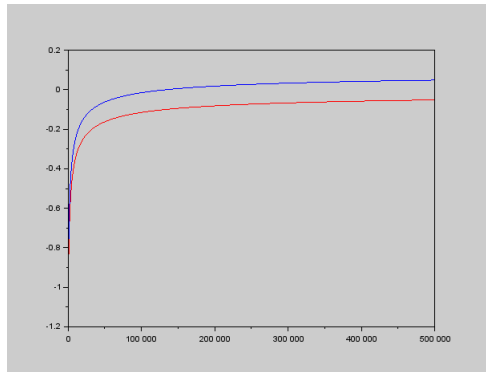
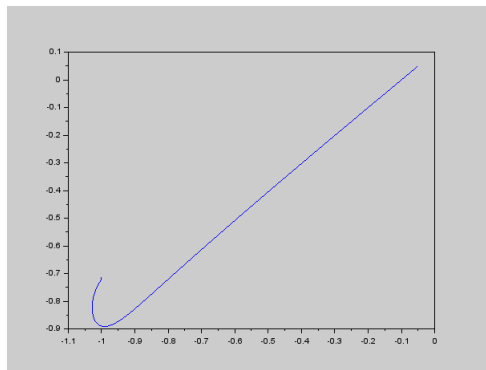
Figure 15: The concentration  $u(0.2)$  and  $v(0.2)$  over timeFigure 16: The concentration  $v(0.2)$  as a function of  $v(0.2)$ 

Next, we take  $\varepsilon = 50$ ,  $b = 1$ ,  $a = 0.1b$ , and  $J = 0.1$ . In this case,  $D = 9(J - \frac{a}{b})^2 + 4(\frac{1}{b} - 1)^3 < 0$ , and Equation 4.4 has a single real solution  $C_1 \simeq 0$ . The solution  $u$  will oscillate around  $C_1$ . Figures 17 and 18 confirm the result of Theorem 5.2, where the solution  $u$  oscillates around  $C_1$ , and the initial conditions  $U_{init}$  and  $V_{init}$  are taken randomly from the interval  $[-1,1]$ .

Figure 17: The concentration  $u(0.2)$  and  $v(0.2)$  over time

Figure 18: The concentration  $v(0.2)$  as a function of  $v(0.2)$ 

Finally, we take  $\varepsilon = 0.1$ ,  $b = 1$ ,  $a = 0.1b$ , and  $J = 0.1$ . In this case,  $D = 9(J - \frac{a}{b})^2 + 4(\frac{1}{b} - 1)^3 < 0$ , and Equation 4.4 has one unique real solution  $C_1 = 0$ . The solution will converge to  $C_1$ . Figures 19 and 20 confirm the result of Theorem 5.1, where the solution  $u$  converges to the constant  $C_1$ . The initial conditions  $U_{init}$  and  $V_{init}$  are taken randomly from the interval  $[-1, 1]$ .

Figure 19: The concentration  $u(0.2)$  and  $v(0.2)$  over timeFigure 20: The concentration  $v(0.2)$  as a function of  $v(0.2)$ 

We take  $\varepsilon = 2$ ,  $b = \frac{100}{99}$ ,  $a = 0.1b$ , and  $J = 0.1$ . In this case,  $D = 9(J - \frac{a}{b})^2 + 4(\frac{1}{b} - 1)^3 < 0$ , and Equation 4.4 has three real solutions:  $C_1 \simeq 0$ ,  $C_2 = 0.1732051$ , and  $C_3 = -0.1732051$ . The solution  $u$  will oscillate around  $C_1$ ,  $C_2$ , or  $C_3$ . Figures 21 and 22 confirm the result of Theorem 5.2, where the



solution  $u$  oscillates around  $C_1$  because the initial condition  $U_{init}(x) = 0.1$  if  $x = 0.5$  else  $U_{init}(x) = 0$  and  $V_{init} = 0$  is closer to  $(C_1, \frac{1}{\varepsilon}(C_1 + a))$ .

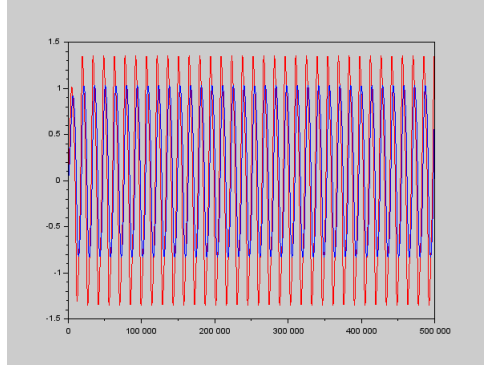


Figure 21: The concentration  $u(0.2)$  and  $v(0.2)$  over time

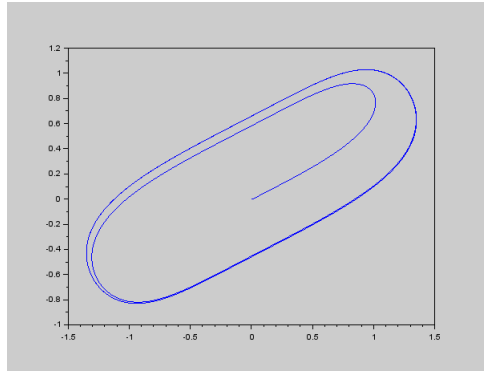


Figure 22: The concentration  $v(0.2)$  as a function of  $v(0.2)$

Notice that the method used above may require a significant amount of time to converge to the solution, especially in two dimensions. To address this issue, we propose a splitting method [26] combined with a domain decomposition method [24,25].

The splitting method allows us to decompose the original problem into smaller, more manageable sub-problems that can be solved individually. This approach can significantly improve computational efficiency and reduce the convergence time. By splitting the equations into different components, such as the diffusion term and the reaction term, we can solve each component separately and combine the solutions to obtain the overall solution.

Furthermore, the domain decomposition method divides the computational domain into smaller sub-domains, which can be solved independently. By solving each subdomain separately and exchanging information at the interfaces, we can obtain the solution for the entire domain. This parallelization technique can further enhance the computational efficiency and speed up the convergence process. By combining the splitting method and domain decomposition method, we can effectively tackle the challenges posed by the high-dimensional nature of the problem and accelerate the convergence to the solution.

## 7. Conclusion

In this study, we delved into the dynamics of a nonlinear reaction-diffusion system characterized by a cubic nonlinearity. This system is of significant interest in various biological contexts, particularly for modeling pattern formation and wave propagation. Our exploration combined theoretical analysis

and numerical simulations to unravel the intricate behaviors of these infinite-dimensional systems. Our unique perspective and methodology set this work apart from previous research, offering novel insights into the underlying dynamics.

Our investigation commenced with an examination of a simplified linear reaction-diffusion system. Subsequently, we unveiled its inherent instability, particularly when subject to small diffusion coefficients. Building upon this foundation, we extended our scrutiny to nonlinear reaction-diffusion systems, pinpointing stability conditions and identifying the emergence of wave patterns under specific parameter regimes. We complemented our theoretical findings with numerical simulations in both one and two dimensions, thereby validating the robustness of our results.

As we look ahead, our research agenda is poised to encompass Networks of FitzHugh-Nagumo dynamical equations, an area with profound implications in neuroscience and cardiac modeling. Our focus will be on characterizing complex phenomena such as spirals, scroll-waves, and intricate patterns, all of which are associated with arrhythmias and are critical for understanding cardiac dynamics. Additionally, we aspire to formulate a comprehensive theory applicable to a broad spectrum of nonlinear reaction-diffusion systems, expanding the horizons of our analysis. Moreover, the exploration of fractional diffusion models as an alternative to classical diffusion mechanisms promises exciting avenues for future inquiry.

In summation, our study enriches the understanding of pattern formation in reaction-diffusion systems, shedding light on fundamental processes in diverse scientific disciplines. It also charts a course for further research in interconnected fields, offering a fertile ground for exploration and discovery.

## References

1. A. L. Hodgkin and A. F. Huxley, A quantitative description of membrane current and its application to conduction and excitation in nerve, *The Journal of Physiology* 117 (1952 aug), no. 4, 500-544.
2. Peter Dayan and L.F. Abott, *Theoretical neuroscience: Computational and mathematical modeling of neural systems*, The MIT Press, 2001.
3. Eugene M. Izhikevich, *Dynamical systems in neuroscience: The geometry of excitability and bursting (computational neuroscience)*, The MIT Press, 2006.
4. Richard FitzHugh, Impulses and physiological states in theoretical models of nerve membrane, *Biophysical Journal* 1 (1961 jul), no. 6, 445-466.
5. John Evans, Nerve axon equations, i: Linear approximations., *Indiana University Mathematics Journal* 21(1971), 877-885.
6. John Evans, Nerve axon equations, ii: Stability at rest., *Indiana University Mathematics Journal* 22 (1972), 75-95.
7. B. Barker, J. Humpherys, G. Lyng, and J. Lytle, Evans function computation for the stability of traveling waves, *Philosophical Transactions of the Royal Society A: Mathematical, Physical and Engineering Sciences* 376 (March 2018), no. 2117, 20170184.
8. Bjorn Sandstede, Stability of travelling waves, *Handbook of dynamical systems*, 2002, pp. 983-1055.
9. Martin Krupa, Bjorn Sandstede, and Peter Szmolyan, Fast and slow waves in the FitzHugh-Nagumo equation, *Journal of Differential Equations* 133 (1997), no. 1, 49-97.
10. C. Jones, N. Kopell, and R. Langer, Construction of the FitzHugh-Nagumo pulse using differential forms, *Patterns and dynamics in reactive media*, 1991, pp. 101-115.
11. Bo Deng, The existence of infinitely many traveling front and back waves in the FitzHugh-Nagumo equations, *SIAM Journal on Mathematical Analysis* 22 (September 1991), no. 6, 1631-1650.
12. B. Ambrosio, Qualitative Analysis of Certain Reaction-Diffusion Systems of the FitzHugh-Nagumo Type, *Evolution Equations and Control Theory*, 2023, 12(6): 1507-1526.
13. J. Jost, *Partial Differential Equations*, Graduate Texts in Mathematics 214.
14. Benjamin Ambrosio, Wave Propagation in an excitable medium. Numerical simulations and analytical approach, *Theses*, 2009.
15. J-L. Lions, *Quelques methodes de résolution des problèmes aux limites non linéaires*, Dunod, 1969.
16. James C. Robinson, *Infinite-dimensional dynamical systems: An introduction to dissipative parabolic pdes and the theory of global attractors (Cambridge texts in applied mathematics)*, Cambridge University Press, 2001.
17. M.D. Angelis, P. Renno, On the FitzHugh-Nagumo model, *Quantitative Biology*, 1202(5783)(2012)1-8.
18. H. Kitano, Biological robustness, *Nat Rev Genet*, 5(2004)826-837

19. Benjamin Ambrosio, Wave Propagation in an excitable medium. Numerical simulations and analytical approach, Theses, 2009.
20. Benjamin Ambrosio and Stanislav M. Mintchev, Periodically kicked feedforward chains of simple excitable FitzHugh–nagumo neurons, *Nonlinear Dynamics* 110 (August 2022), no. 3, 2805–2829.
21. J.M. Ortega and W.C. Rheinboldt, Iterative solution of nonlinear equations in several variables, Academic Press, San Diego, 1970. Reprinted as vol. 30, *Classics in Applied Mathematics*, SIAM, Philadelphia, 2000.
22. L. perko. differential equations and dynamical systems, Text in Applied Mathematics, 7. Third edition, Springer.
23. Hecht, F. (2012). New development in FreeFem++. *Journal of numerical mathematics*, 20(3-4), 251-266
24. M.R. Amattouch, N. Nagid, H. Belhadj. Optimized Domain Decomposition Method for Non Linear Reaction Advection Diffusion Equation. *European Scientific Journal* , Vol 12, No 26 (2016).
25. M.R. Amattouch, H. Belhadj. Combined Optimized Domain Decomposition Method and a Modified Fixed Point Method for Non Linear Diffusion Equation. *Applied Mathematics and Information Sciences*, 11, No. 1, 201-207 (2017).
26. M.R. Amattouch, N. Nagid, H. Belhadj, a new splitting method for the Navier Stokes equation , *Journal of space exploration*, Vol 2, 24 august 2017.

*Amattouch M.R.,  
 Department of Mathematics and Computer Science Department,  
 University Abdelmalk Essaadi, National School of Applied Sciences,  
 Al hoceima.  
 Morocco.  
 E-mail address: mohamedridouan.amattouch@fstm.ac.ma*